

## OVERVIEW OF THE QUEENSLAND CLOUD SEEDING RESEARCH PROGRAM

Sarah A. Tessendorf<sup>1\*</sup>, Roelof T. Brintjies<sup>1</sup>, Courtney E. Weeks<sup>1</sup>, Michael Dixon<sup>1</sup>,  
Matthew Pocerich<sup>1</sup>, James W. Wilson<sup>1</sup>, Rita D. Roberts<sup>1</sup>, Edward A. Brandes<sup>1</sup>, Kyoko Ikeda<sup>1</sup>,  
Charles A. Knight<sup>1</sup>, Louise Wilson<sup>2</sup>, Justin R. Peter<sup>2,3</sup>, Nicole Torosin<sup>1</sup>

<sup>1</sup>National Center for Atmospheric Research, Boulder, CO

<sup>2</sup>Monash University, Melbourne, VIC, Australia

<sup>3</sup>Queensland Climate Change Centre of Excellence, Indooroopilly, QLD, Australia

**ABSTRACT.** As a response to water shortages in Southeast Queensland brought about by reduced rainfall and increasing population, the Queensland government decided to explore the potential for cloud seeding to enhance rainfall. A cloud seeding feasibility study was conducted in the Southeast Queensland region December 2007–March 2008 and again from October 2008–February 2009. In both seasons of the field effort, radar measurements and in situ aircraft microphysical data were collected and an exploratory randomized seeding study was initiated. Climatology analyses established the weather regimes responsible for the regional rainfall. Results indicate that most deep convection in the region has a strong warm rain formation component, except for early summer storms with higher cloud bases. Initial statistical analyses of the randomized seeding experiment suggest that hygroscopic seeding may potentially increase rainfall, consistent with previous experiments; however, the robustness of the results is limited by the small sample size.

### 1. INTRODUCTION

Water shortages in Southeast Queensland (SEQ), Australia prompted the Queensland government to seek ways to create more water resources. As a response, the Queensland Cloud Seeding Research Program (CSRP) was conducted to investigate the feasibility of precipitation enhancement via cloud seeding.

Scientists from the National Center for Atmospheric Research (NCAR), the South African Weather Service (SAWS), the University of Witwatersrand (WITS), and Weather Modification Inc. (WMI), in collaboration with the Australian Bureau of Meteorology (BoM), Monash University, the University of Southern Queensland (USQ), the Centre for Australian Weather and Climate Research (CAWCR), and MIPD Pty Ltd, conducted the feasibility study for rainfall enhancement via cloud seeding during the summer rainfall regime. The CSRP feasibility study included a variety of measurement systems, some using novel technologies. A unique component of this study was a dual-polarization, dual-wavelength Doppler weather research radar (CP2). This multi-parameter radar also contributed to dual-Doppler radar coverage. This is noteworthy in that the evolution of microphysical precipitation characteristics, such as particle type, number, and size, within a seeded cloud can be related to the airflow patterns within the cloud.

The potential for man-made increases in precipitation strongly depends on the natural microphysics and dynamics of the clouds that are seeded. Further, these factors can differ significantly from one geographical region to another, as well as during and between seasons in the same region. Hence, an evaluation of the climatology of clouds and precipitation in the SEQ region was a necessary part of this feasibility study. For example, in some instances clouds may not be amenable to seeding, or the frequency of occurrence of suitable clouds may be too low to warrant the investment in an operational cloud seeding program.

Another important part of this feasibility study was to obtain high-quality measurements that pertain to cloud and precipitation processes. Aerosol and microphysical measurements, in particular, help determine if seeding could be beneficial and also what the optimal seeding method would be with regard to enhancing precipitation in local clouds. Thus, microphysical and dynamical studies of naturally forming clouds were an integral part of the study.

Cloud seeding techniques also need to be evaluated using a randomization procedure to demonstrate statistically if the seeding method works to enhance rainfall and to quantify any potential enhancement. The randomized experiment conducted in the Queensland CSRP was exploratory; if the CSRP results indicate that cloud seeding is feasible, then a confirmatory randomized statistical experiment should become the next phase of a future program.

---

\*Corresponding Author: S.A. Tessendorf, Research Applications Laboratory, National Center for Atmospheric Research, P.O. Box 3000, Boulder, CO 80307. saraht@ucar.edu

Typically, the statistical evaluation of cloud seeding experiments has relied on radar-derived precipitation flux, storm water mass, duration, and size. However, the very large natural variability in storms can mask cloud seeding effects. Consequently, a large sample size of randomized seeded and unseeded cases is required to obtain statistical significance at a high confidence level. Even then, in the absence of physical measurements, there is uncertainty in the true understanding of physical mechanisms that were responsible for any seeding effect suggested by the statistical analysis. This project was undertaken in the hopes that through the use of physical measurements, such as from aircraft and a multi-parameter radar, microphysical processes could be more directly observed, making it possible to understand cause and effect seeding relationships, thus not having to solely rely on statistical means that have often generated controversy.

Analysis efforts for the Queensland CSRP were therefore focused on three issues: understanding the weather and climate, characterizing the atmospheric aerosol and its relation to cloud microphysics, and assessing the impact of cloud seeding on microphysical and dynamical processes in clouds to enhance rainfall. The data sets collected in the two field seasons are vast and unique for cloud seeding research, and thus will support a variety of research efforts. The purpose of this paper is to present an overview of the Queensland CSRP experiment. The program design describes the facilities and research goals of the project, as well as some initial climatology results, in Section 2. A summary of the field operations is provided in Section 3, and includes some results from the aircraft measurements and statistical analysis. Section 4 outlines some unique opportunities that utilize the dual-polarization and dual-Doppler radar data, but analysis of these data is still ongoing. Conclusions and future work are summarized in Section 5.

## 2. PROGRAM DESIGN

The region of Southeast Queensland (SEQ), which includes the city of Brisbane and the Sunshine and Gold Coast regions north and south of the city, was targeted for the field effort (Fig. 1). Two seasons of field operations were conducted to assess the feasibility of both hygroscopic (Mather et al. 1997, Foote and Brintjes 2000) and glaciogenic (e.g., Rosenfeld and Woodley 1993, Levi and Rosenfeld 1996) cloud seeding methods. Operations took place from December 2007–March 2008 in season one, and from November 2008–February 2009 in season two.

### 2.1 Facilities

Facilities employed during the Queensland CSRP are key to what made this cloud seeding experiment different from previous experiments. In addition to traditional radar measurements, the Queensland CSRP included dual-polarization, dual-wavelength, and dual-Doppler radar capabilities. Furthermore, an extensive suite of aircraft instrumentation was used to collect in situ cloud microphysical and aerosol measurements, and disdrometers were deployed at the surface to aid in radar calibration. Each element of the field effort is described in more detail in the following sections.



*Figure 1. Map of Southeast Queensland region targeted for the Queensland CSRP field effort and associated facilities and landmarks. The 30-degree beam crossing angle dual-Doppler lobes are overlaid in black.*

#### 2.1.1 Radar

The Australian Bureau of Meteorology (BoM) operates a network of surveillance weather radars in the SEQ region (Table 1). Most of these weather radars operate at 10 cm (S-band) wavelength and complete a volume scan every 10 min. The Marburg and Mt Stajylton radars are the two radars closest to the CSRP operations (Fig. 1). The Mt Stajylton radar also has Doppler capabilities and is the only network radar that operates on a 6-min volume scan cycle. Data from the five BoM network radars described in Table 1 were merged into a mosaic reflectivity product, which provided coverage over the full SEQ region.

The CP2 radar, originally developed and owned by NCAR, was obtained by the BoM in 2007 and installed at Redbank Plains to the southwest of

Brisbane (Fig. 1; Keenan et al. 2006). CP2 is actually two co-located radars, the main radar being an S-band (10 cm) unit and the smaller radar being an X-band (3 cm) unit. The X-band antenna piggybacks on the main S-band antenna (Fig. 2b) and is designed to view the same sample volume as the S-band radar. The technical characteristics of CP2 are described by Bringi and Hendry (1990).

The CP2 radar scanning strategies for the Queensland CSRP were designed to meet three main objectives: (1) obtain statistics of rainfall in

SEQ storms, (2) monitor storm microphysical characteristics in support of in situ observations, and (3) gather sufficient observations of precipitation initiation in both seeded and unseeded storms to document the evolution of microphysical precipitation formation processes in these storms. The BoM network radars operated in a regular volume scanning mode (full 360 degree azimuth scans) and as such provided adequate data for statistical rainfall studies (Objective 1). Special CP2 scanning strategies were designed to meet the remaining radar objectives.

**Table 1.** General specifications for the Bureau of Meteorology radars located in/near the Southeast Queensland region.

Site	Latitude (deg)	Longitude (deg)	Type	Wavelength	Scan interval
Grafton	29.620 S	152.970 E	WSR 74S	10 cm	10 min
Moree	29.500 S	149.850 E	WF100C	5 cm	10 min
Mt Stapylton	27.718 S	153.240 E	Gematronik Doppler	10 cm	6 min
Marburg	27.610 S	152.540 E	EEC WSR 74S	10 cm	10 min
Mt Kanigan	25.957 S	152.577 E	EEC DWSR 8502S	10 cm	10 min

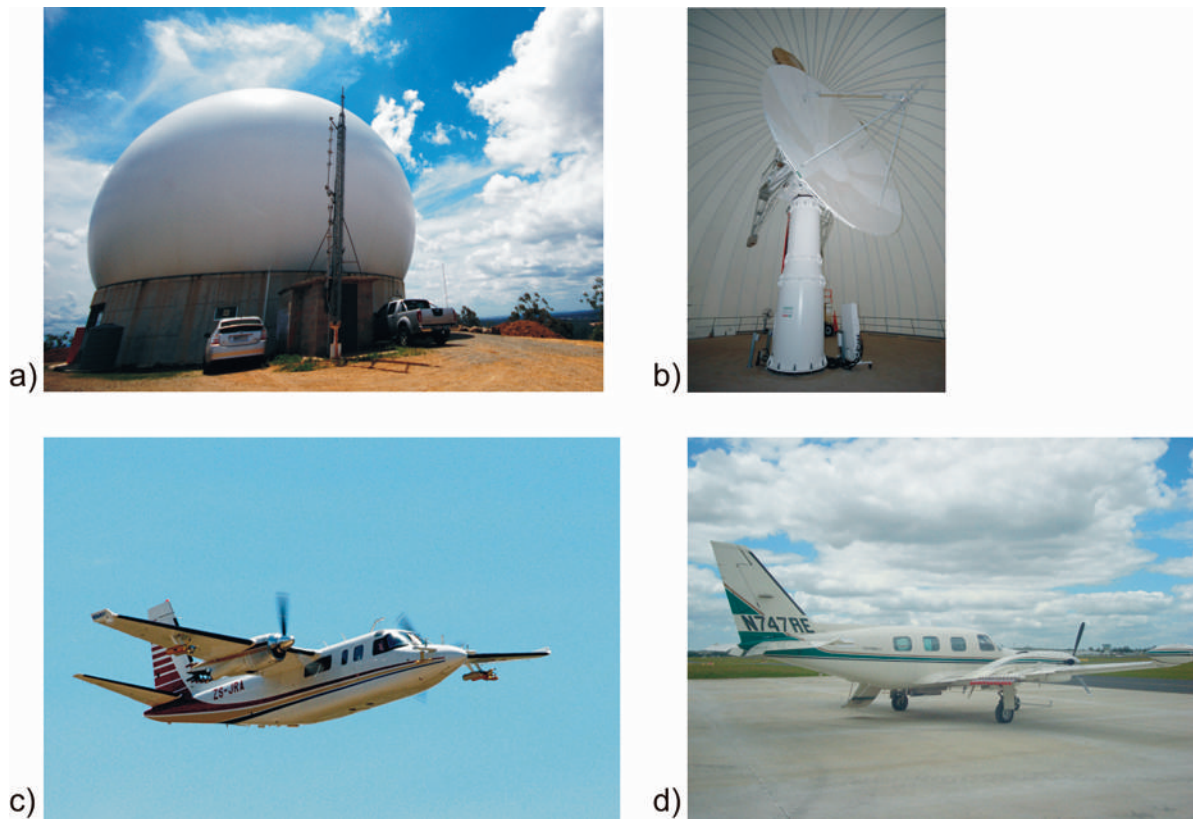


Figure 2. CP2 site infrastructure at Redbank Plains: (a) Antenna and pedestal are within an inflated radome mounted over housing for office, storage and transceiver, and (b) CP2 S-band and X-band antennae (right) [Photos courtesy Scott Collis/CAWCR], and photos of the (c) the SAWS Aerocommander research/seedling aircraft in flight on a research mission [Photo courtesy Scott Collis/CAWCR], and (d) WMI Piper Cheyenne II seeding aircraft highlighting the wing-mounted flare racks [Photo courtesy Sarah Tessendorf/NCAR].

When unattended, CP2 operated in a volume-scan mode, synchronized with Mt Stapylton for dual-Doppler analysis capabilities, which produced a volume of Plan Position Indicator (PPI) sweeps once every six minutes. During field operations, CP2 was operated in a PPI or Range Height Indicator (RHI) sector-scan mode, in which designated azimuth sectors were scanned with PPI sweeps or RHI scans. Sector scanning allowed high resolution of designated storms. When seeding operations were underway, the CP2 radar scans followed the targeted cell for at least 20 minutes after seeding ended to capture any initial microphysical responses before scanning another declared case. If the targeted cell was within the dual-Doppler lobes, then CP2 aimed to scan it for an additional hour after seeding ended to capture any dynamic responses (see Fig. 1). If no other cells were declared in the interim, CP2 would scan the most recently targeted cell through its dissipation. Other scanning strategies employed by the CP2 radar included vertically pointing scan sequences during light rain and low-level (0.5 and 1.0 degree elevation) small sector scans over the disdrometer site. These scans were used to evaluate the radar hardware calibration and to verify radar-derived rain drop size distributions.

### 2.1.2 Aircraft

Two aircraft were used during the first season of the project: one was primarily a research aircraft, but also served as a secondary seeding aircraft if conditions warranted; the second aircraft was the primary seeding aircraft. In season two, only the research aircraft was available and it also served as the seeding aircraft. The research aircraft was the South African Weather Service (SAWS) Aerocommander (ZS-JRA; Fig. 2c). It carried flare racks on each wing (10 burn-in-place hygroscopic or silver iodide flare capacity each) and had a full suite of atmospheric instrumentation described in detail below. In season one, the Weather Modification Inc (WMI)/MIPD Piper Cheyenne II (N747RE; Fig. 2d) served as the primary seeding aircraft. It carried flare racks on each wing (12 burn-in-place hygroscopic or silver iodide flare capacity each) and an undercarriage ejectable silver iodide flare rack (306 flare capacity).

The research aircraft had a suite of instruments capable of taking trace gas, aerosol, and microphysical measurements in seeded and unseeded clouds (see Table 2 for a list of instrumentation on board in each season). All instruments were monitored by an in-flight scientist and maintained by a technician to ensure proper function. Data quality checks were routinely performed to assess instrument performance and diagnose maintenance needs. The full suite of instruments provided multiple

measurements of key microphysical parameters and allowed for intercomparison measurements to assess instrument performance and data quality.

Aircraft operations were based at Archerfield Airport, where daily weather and flight planning briefings were held for the pilots (see Fig. 1). During flights, operations were coordinated via radio communications between the pilots and the Operations Director at the CP2 radar facility, which served as the Operations Center (see Fig. 1). Both the Operations Center and the airport hangar office had phone and high speed internet connections to enable communications and data transfer/archival between the two sites, as well as off site (i.e., NCAR).

### 2.1.3 Surface measurements

Raindrop measurements were made with disdrometers installed at a ground site roughly 16 km from the CP2 radar. In season one, a two-dimensional video disdrometer (2DVD), owned and operated by NCAR, was deployed. Three disdrometers were available for season two: a 2DVD and an impact disdrometer owned by the BoM and a Particle Video Imager developed by NASA. The ground-based raindrop measurements were used to help calibrate the CP2 radar, establish drop size distribution (DSD) characteristics of stratiform and convective rains and radar-derived microphysical relationships, and to develop procedures for monitoring drop size distributions in seeded and unseeded clouds with polarimetric radar.

## 2.2 Research goals and procedures

### 2.2.1 Climatology analyses

The first objective in this feasibility study was to understand the local precipitation climatology, including weather patterns and conditions that drive convection, in order to put the cloud seeding and precipitation process analyses into context, as well as to determine the frequency of clouds suitable for seeding. These analysis efforts include building climatologies of radar and rain gauge data, synoptic weather patterns, thermodynamic soundings, and relationships of climate indices (i.e., Southern Oscillation Index) with precipitation in the region. Five years of Marburg radar data were examined to determine the climatology of storm initiation location, size, storm top height, and duration (Peter et al. 2010). This was combined with a k-means statistical clustering analysis (Hartigan and Wong 1979) that used thermodynamic sounding data (i.e., instability, wind, and moisture flux parameters) to characterize the synoptic regimes that accounted for the observed rainfall (from radar and rain gauge data).

**Table 2.** List of instrumentation on SEEDA1 in each season of the Queensland CSRP.

Instrument	Purpose/Comment	Range	Season
<b>State Variables</b>			
Rosemount Temperature, Static and Dynamic Pressure, and GPS	Temperature, pressure, altitude, TAS, and location (SAWS)	<i>multiple</i>	Both
Edgetech Dew point sensor	Moisture content (NCAR)	-40° to 60°C	2
Vaisala Temperature and Relative Humidity	Secondary temperature and moisture content (SAWS)	-50° to 50°C, 0–100%	Both
AIMMS-20 probe	Temperature, relative humidity, pressure, three-dimensional wind components	<i>multiple</i>	Both
<b>Cloud Physics</b>			
PMS FSSP	Cloud droplet spectra (SAWS)	0.5–47 µm	1
DMT SPP-100 FSSP	Cloud droplet spectra (SAWS)	0.5–47 µm	Both
PMS 2D-C	Small precipitation particle size, concentration and shape (SAWS)	25–800 µm	1
PMS 2D-P	Large precipitation particle size, concentration and shape (SAWS)	200–6400 µm	1
DMT CIP	Small precipitation particle size, concentration and shape (NCAR; part of CAPS probe listed below)	25–1550 µm	Both
DMT PIP	Large precipitation particle size, concentration and shape (NCAR)	100–6200 µm	2
PMS Hot-wire (King) Liquid Water Content (LWC) Probe	Liquid water content (SAWS)	0.01–3 g m <sup>-3</sup>	Both
DMT CAPS probe	Aerosol through precipitation size spectrometer; LWC; CIP; static and dynamic pressure; temperature (NCAR)	<i>multiple</i>	Both
<b>Aerosols</b>			
DMT CCN Counter	Cloud condensation nuclei concentration and spectra (WITS)	Depends on supersaturation	Both
Texas A&M DMA	Fine mode aerosol spectra and concentration (NCAR)	0.01 to 1 µm	Both
PCASP	Aerosol concentration and spectra (WITS)	0.1 to 3 µm	1
DMT SPP-200 PCASP	Aerosol concentration and spectra (WITS)	0.1 to 3 µm	2
ASU Aerosol Particle Sampler	Aerosol chemical composition (NCAR)	N/A	Both
<b>Trace Gases</b>			
TECO SO <sub>2</sub> (43c)	Sulfur dioxide (WITS)	0–100 ppm	Both
TECO O <sub>3</sub> (49i)	Ozone (WITS)	0–200 ppm	Both
TECO NO <sub>y</sub> (42c)	Nitrogen oxides (NCAR)	0–100 ppm	Both
TECO CO (48c)	Carbon monoxide (WITS)	0–10,000 ppm	1
<b>Cloud and Situation Imagery</b>			
Digital still camera	To show development of clouds and treatment situations for historical purposes	N/A	Both

A cluster analysis was performed using 00Z radiosonde data from the Brisbane Airport for the period 1 January 1990 to 31 December 2008. Seven regimes were identified: three separate southeasterly regimes, three westerly regimes, and an easterly regime. The analysis clearly illustrates the seasonality of rainfall regimes. The seasonal rainfall cycle has low monthly totals in the winter months and high totals in the summer months, as expected, with November–February being the wettest months (Fig. 3). During the summer, the easterly and

westerly regimes contribute much of the monthly rainfall (E and W, respectively, in Fig. 3), and combined yield nearly half of the annual rainfall (Table 3). The northwesterly regime (NW, in Fig. 3) also makes important contributions to annual rainfall (22%), mostly during the summer, despite only occurring 6% of the time. The southeasterly ‘dry’ and southwesterly regimes occur most exclusively during winter and do not make any sizeable contributions to rainfall in any month (SE (d) and SW, respectively, in Fig. 3).

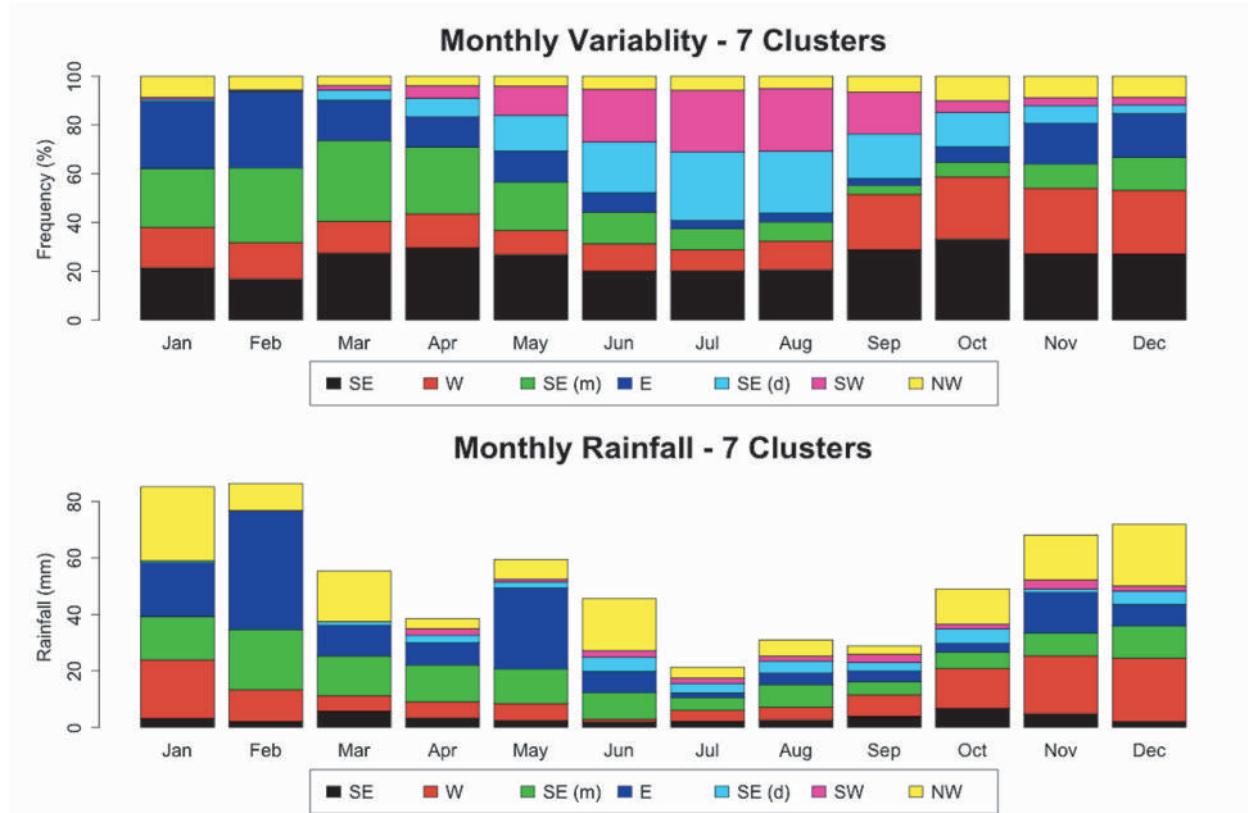


Figure 3. Monthly distributions of the 7-cluster synoptic regimes’ (top) frequency of occurrence and (bottom) contribution to annual rainfall.

Table 3. Abbreviation (Abbr.), annual frequency (rounded to nearest whole percentage), contribution to rainfall, and a brief description for each of the seven synoptic clusters.

Regime	Abbr.	Frequency (%)	Rainfall (%)	Description
Southeasterly	SE	25	6	SEly, low moisture flux (mflux); all months
Southeasterly moist	SE (m)	16	21	SEly, high mflux; summer
Southeasterly dry	SE (d)	13	5	SEly, low mflux, high shear; winter
Easterly	E	13	23	Ely, moderate mflux, high total water; summer
Westerly	W	17	20	Wly, high mflux; all months
Southwesterly	SW	11	3	SWly, low mflux, low total totals; winter
Northwesterly	NW	6	22	NWly, high mflux; summer

The most frequent regime, accounting for roughly a quarter of all days (Table 3) and regularly occurring throughout the year, is southeasterly (SE, in Fig. 3). The SE regime is characterized by a southeasterly moisture flux and moderate instability and shear, and does not contribute significantly to the total rainfall in any month. A 'moist' southeasterly trade regime (SE (m), in Fig. 3) accounts for 16% of all days and occurs most frequently during the late summer, although it still accounts for approximately 10% of days during the winter months. This regime contributes 21% of rainfall during all months of the year and is characterized by strong southeasterly moisture flux and moderate atmospheric moisture and instability (Table 3). A key feature of the sounding in this regime is the trade inversion at about 800 hPa and high moisture up to approximately 500 hPa.

### 2.2.2 Aerosol and microphysics studies

Since the primary goal of this project was to ascertain if cloud seeding is a feasible means for enhancing rainfall in the SEQ region, analyses to study the effects of cloud seeding are paramount. While the effects of seeding are often mostly based on randomized seeding statistical analyses, it is also important to gain a good *physical* understanding of natural cloud microphysical and precipitation processes and potential seeding effects to be able to explain and support the statistics. Therefore, in order to fully understand the effects of cloud seeding, a working knowledge of the natural precipitation processes in the region is vital, including the environmental conditions that influence cloud microphysics (such as sub-cloud aerosol particles). Specific analysis efforts include characterizing the ambient aerosol conditions and initial cloud base DSDs in natural and seeded clouds and studying the evolution of drop growth and ice crystal formation through the mixed-phase region in deep convection via in situ cloud microphysics measurements.

In order to collect measurements for the aerosol and microphysical studies, several standardized research flight plans were implemented. In season one, when there were two aircraft, the seeding aircraft spent its flight time at cloud base searching for hygroscopic seeding candidate clouds and burning flares on declared cases, while the research aircraft spent time in cloud above the seeding aircraft penetrating key levels of interest or collecting sub-cloud aerosol measurements. Such aerosol measurements included surveys in the sub-cloud layer to look for any gradients in aerosol from the coastline to further inland, and aerosol and cloud condensation nuclei (CCN) measurements at cloud base.

In season two, the standardized research flight plans were modified slightly due to having a single aircraft for both seeding and research. In this vein, every flight aimed to collect cloud base aerosol (just below cloud base) and cloud base droplet spectra measurements (1000 ft above cloud base) before attempting other flight objectives. If the flight was declared a randomized seeding mission, then immediately after each randomized case (seed or no seed), cloud base penetrations (1000 ft above cloud base) were performed to measure the initial droplet spectra before continuing to the next case or research objective. If the flight was a cloud microphysics research mission, then cloud base aerosol measurements and cloud penetrations at key levels were conducted including 1000 ft above cloud base, the freezing level, and  $-5^{\circ}\text{C}$  and  $-10^{\circ}\text{C}$  levels. Often flights had both seeding and research objectives. We attempted to collect a large sample of cloud base droplet spectra in seeded and unseeded clouds for a statistical comparison of the initial DSDs and to understand mixed-phase microphysical processes.

The goals of the aerosol and microphysics studies are to determine the naturally occurring aerosol and droplet size spectra and how they affect precipitation processes, such as warm rain formation and mixed phase processes. From these studies we hope to determine whether hygroscopic or glaciogenic seeding would make these clouds more efficient.

### 2.2.3 Cloud seeding assessment studies

Statistical analysis provides a first glance at potential effects of seeding and offers guidance for important physical analysis of the data to interpret the statistical results. The SEQ CSRP statistical randomized seeding experiment was very similar to those conducted previously in South Africa and Mexico (Foote and Buintjes 2000). As in the earlier experiments, the selection criteria for the Queensland CSRP statistical analysis required that randomized cases have a 35 dBZ threshold TITAN track (Dixon and Weiner 1993) for greater than two volume scans and a maximum storm volume (defined as the volume of the storm with reflectivity greater than the 35 dBZ TITAN threshold) less than  $750\text{ km}^3$  (Mather et al. 1997). The Mt Stapylton radar was used for the TITAN tracking of the randomized cases and determination of whether each case met the criteria for inclusion in the statistical analysis.

For the Queensland CSRP randomized experiment, only hygroscopic seeding was conducted; however, some non-randomized trials with glaciogenic seeding were performed during the project. Randomized

cases were declared by the pilots of the seeding aircraft when a rain-free, uniform, and dark cloud base at least roughly 2 km in diameter was located optimally within 100 km of the CP2 radar and within the Mt Stapylton domain, with an approximate updraft of at least 200 ft/min. We also required a minimum of 20 km separation between randomized cases in order to avoid contamination among the cases. A 35-dBZ TITAN track was not a requirement for declaring a randomized case in the CSRP, but as was mentioned above was required at some point during its evolution for the case to be included in the statistical analysis. A pseudo-random sequence of decision envelopes was created by joining together blocks of evenly balanced random sets of decisions. This was done to prevent excessively long strings of identical decisions, which will occur in a truly random series of binomial events (Cleveland 1978). For each case declaration, the next sequential randomized envelope was opened at the CP2 Operations Center and the decision was communicated to the pilots via radio. For seed decisions, three to four sets of 2 flares (one on each wing) were burned consecutively depending on the length of each burn to achieve roughly 15 minutes of consecutive flare burn time. In cases where the updraft diminished during seeding, the seeding was stopped after the current set of flares completed burning. For no seed decisions, the seeding aircraft circled at cloud base for 5 minutes to mark the case location before undertaking the next mission objective.

The goal of the randomized seeding statistical analysis is to quantify the effects of hygroscopic cloud seeding on storm properties (size, duration) and rainfall production. Furthermore, these cloud seeding assessment studies aim to understand the microphysical effects that seeding with hygroscopic or glaciogenic material has on clouds in Southeast Queensland. A key part of this objective is to establish new methods to study the physical effects of seeding, especially those that utilize advanced radar and measurement technologies. This topic will be further explored in Section 4.

### 3. SUMMARY OF FIELD OPERATIONS

#### 3.1 Aircraft research

Aircraft-based research operations began in earnest on 12 January 2008 in season one and 4 November 2008 in season two. The two seasons had a total of 108 flight operation days with 164 total flights. Of the total flights, there were 142 research flights. In season one, 49 research flights were flown by the research aircraft and 39 by the seeding aircraft, while in season two, all operations were conducted by the research aircraft and they flew 54 research flights. These flights comprised 386 total

flight hours. In each season the research aircraft flew 150 hours and in season one the seeding aircraft flew 86 hours.

Out of the total research flight segments in each season, there were relatively more cloud base aerosol measurements in season two, while season one operations were more dominated by warm cloud penetrations (above cloud base yet below the freezing level; Fig. 4). Season two had relatively more penetrations in the freezing and mixed-phase levels, instead of focusing on the warm cloud region. This was partially due to the type of convection that occurred predominantly in each season (more deep mixed-phase convection occurred in season two) and a shift in the flight mission objectives (see Section 2.2.2). Furthermore, since the research aircraft also performed hygroscopic cloud seeding in season two, it resulted in more flight time spent at cloud base, whereas in season one it spent more time in cloud above the seeding aircraft that was seeding at cloud base.

From the frequent and regular cloud base measurements collected by the research aircraft in season two, a summary of the cloud base aerosol

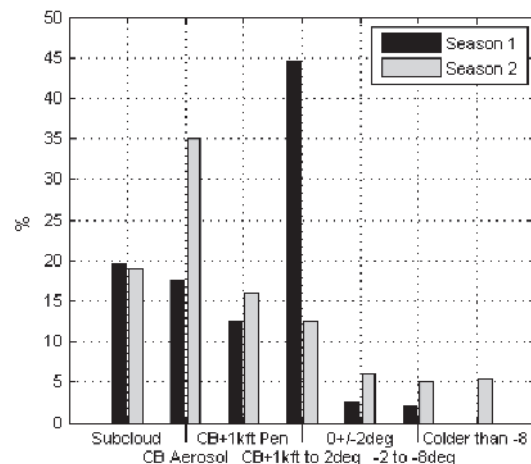


Figure 4. Frequency of SEEDA1 flight heights relative to cloud base (CB) for both seasons. The percentage is the fraction of all flights for each season that fell into the given height range: "Subcloud" = any height below cloud base, "CB Aerosol" = at (but just below) cloud base (out of cloud) for aerosol and CCN measurements, "CB + 1kft Pen." = cloud base penetrations made around 1000 ft above cloud base, "CB+1kft to 2deg" = warm cloud penetrations above the initial cloud base penetration yet warmer than the freezing level, "0 +/- 2deg" = penetrations taken within 2°C of the freezing level, "-2 to -8deg" = penetrations taken between -2° and -8°C, "Colder than -8deg" = penetrations taken at temperatures less than -8°C.



conditions has been compiled, and studies to characterize the various aerosol conditions are underway. One effort has focused on how the aerosol varies by source region, and thus back trajectories were calculated using the Hybrid Single-Particle Lagrangian Integrated Trajectory (HYSPLIT) model (Draxler and Hess 1998). The Global Data Assimilation System (GDAS) archived data, with a temporal resolution of three hours and gridded to 1 degree x 1 degree in latitude and longitude, was used to calculate the back trajectories. The GDAS data set is the only one available that covers the CSR project domain for the entire duration of the measurements; however, comparisons between trajectories calculated using GDAS and other data sets for the same region in past years yielded similar results (not shown). The back trajectories were calculated for 48 hours ending at every cloud base measurement location, altitude, and time. The trajectories were then grouped into regimes with similar paths based on the time each trajectory spent in quadrants relative to Brisbane: ocean (or land) north or

south of the city. The regimes were grouped by first determining if each trajectory spent the majority of its time over ocean or land, then it was assigned to which of the two ocean (or land) quadrants it spent the most time within (Fig. 5a).

The PCASP (Passive Cavity Aerosol Spectrometer Probe; see Table 2) aerosol concentrations at cloud base were observed to vary from clean ( $100 \text{ cm}^{-3}$ ) to more polluted ( $1500 \text{ cm}^{-3}$ ), with the maritime HYSPLIT trajectory regimes (easterly, E, and northeasterly, NE) being the cleanest (Fig. 5b). Likewise, the maritime regimes exhibited the lowest 0.3% supersaturation CCN concentrations, often less than  $300 \text{ cm}^{-3}$ , while the CCN concentrations in the continental flow regimes (westerly, W, and northwesterly, NW) ranged from 200-600  $\text{cm}^{-3}$ , still relatively clean compared to CCN concentrations measured in highly polluted regions (Andreae 2008).

The cloud base temperatures from the aircraft measurements for the two seasons when the aircraft

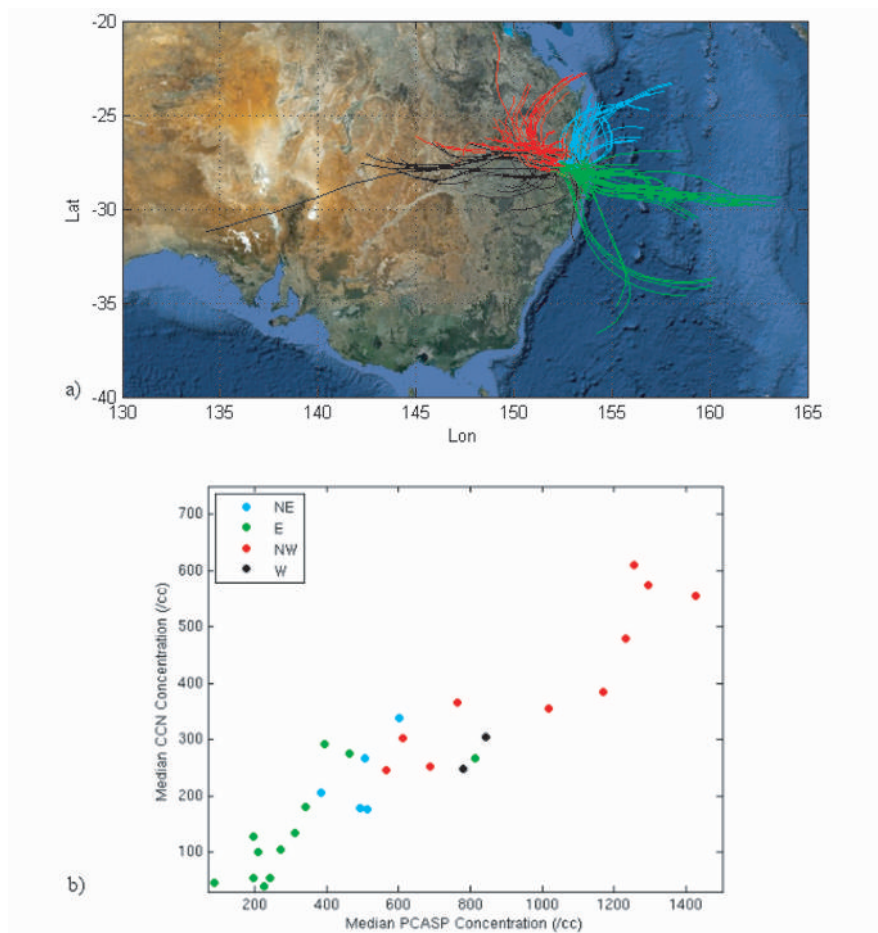


Figure 5. a) Map of HYSPLIT back trajectories colored by the quadrant (or HYSPLIT regime) it spent the most time in, and b) scatter plot of the median PCASP concentration versus the median 0.3% supersaturation CCN concentration per cloud base segment with colors corresponding to the HYSPLIT regime the measurement was assigned to (see legend).

were flying are displayed in Figure 6. Although there are large variations, there is a general tendency for cloud bases to be higher, at cooler temperatures, during the early part of the summer season and for lower and warmer bases as the season progresses. The lower cloud bases in the latter part of the season also provide for a deeper layer of the cloud warmer than  $0^{\circ}\text{C}$  (not shown). The depth of the “warm” cloud layer is important because this will determine in many instances if coalescence will be active and large drops present before the cloud top reaches temperatures colder than  $0^{\circ}\text{C}$ . This certainly impacts the efficiency of the ice processes in the cloud and could also affect precipitation production.

During the second season of the Queensland CSRP, the aircraft took measurements in the tops of newly developing turrets of deep convective mixed-phase clouds on at least 18 different days. To date, we have studied the in situ measurements on six of these days in detail. On four of the studied days, in natural (unseeded) clouds, the aircraft measured large drizzle-sized drops (diameters  $>300\ \mu\text{m}$ ) in the growing cloud turret tops near the  $0^{\circ}\text{C}$  level. The cloud bases in these cases ranged from 700 to 1200 m MSL. The natural clouds on two of these days showed evidence that graupel had formed around the  $-5^{\circ}\text{C}$  level, and subsequently a secondary ice process (ice multiplication; Hallet and Mossop 1974) evolved. The microphysical cloud data from a case in which ice multiplication was observed (27 January 2009) is shown in Figure 7, while the same for a case (20 November 2008)

without the presence of large drops at the freezing level (and thus no subsequent ice formation at temperatures warmer than  $-12^{\circ}\text{C}$ ) is presented in Figure 8. The two days studied with clouds that did not exhibit large drops at the freezing level were both observed in November 2008, in the early part of the season when cloud bases were generally higher (Fig. 6). The cloud bases in those cases ranged from 1500 to 2400 m MSL. It is possible that during the early part of the season, when cloud bases are generally higher (and thus colder), coalescence does not occur before reaching mixed-phase conditions, ice multiplication may not occur, and first ice may only form at temperatures colder than  $-12^{\circ}\text{C}$ . Hygroscopic seeding may be more effective in these clouds providing for earlier coalescence and possibly the onset of a more efficient ice process. Future analyses will study the remainder of the mixed-phase in situ measurements in more detail and also focus on the ice formation processes in seeded clouds to investigate if there is evidence of more efficient warm rain and ice formation processes in such cases.

At times, deep stratiform systems are observed in the region and in those that we collected in situ measurements the natural precipitation processes were very efficient, with very little (if any) supercooled liquid water and much ice evident at sub-freezing temperatures (not shown). This suggests that neither hygroscopic nor silver iodide seeding would have a precipitation enhancement effect in such highly efficient systems.

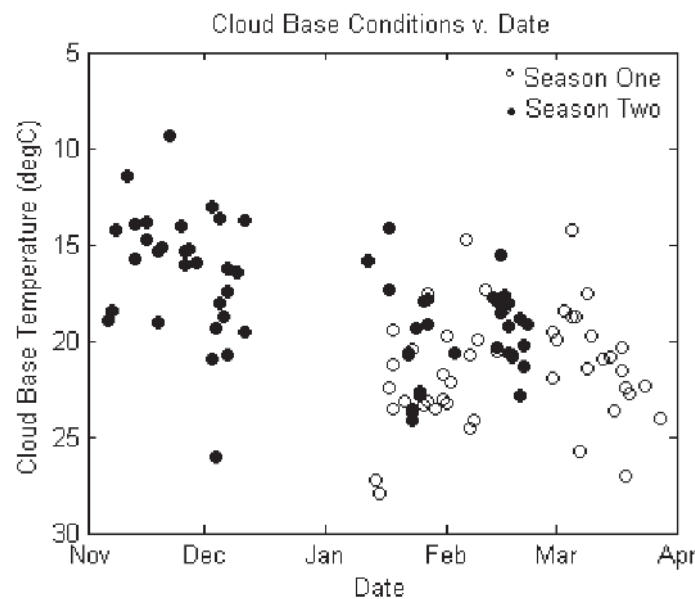


Figure 6. Cloud base temperatures as a function of the date during the field season (2007–2008 and 2008–2009 seasons).

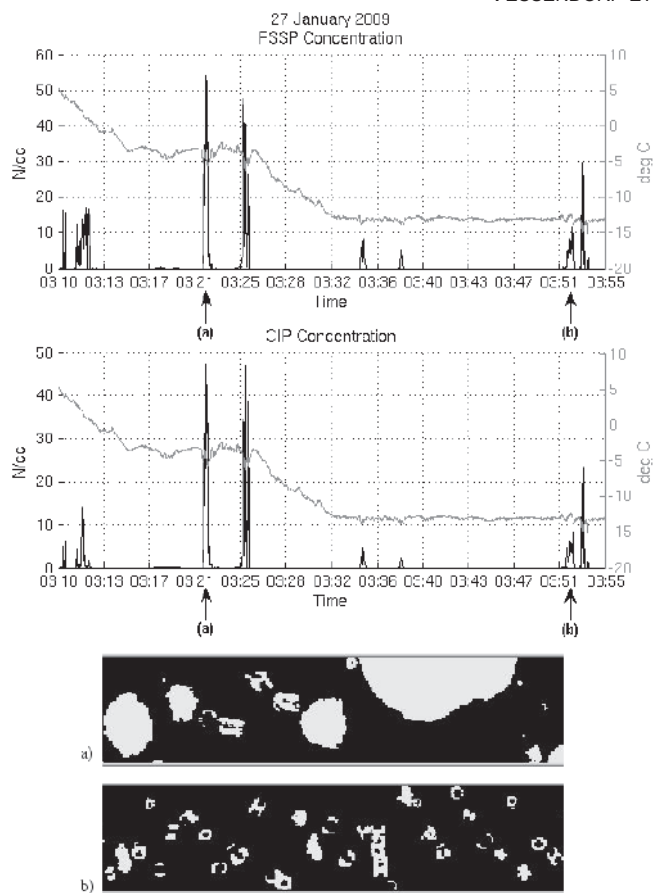


Figure 7. Time histories for FSSP droplet concentration ( $\text{cm}^{-3}$ ) and CIP particle (larger than  $40 \mu\text{m}$  diameter) concentrations ( $\text{cm}^{-3}$ ) with temperature ( $^{\circ}\text{C}$ ) overlaid in gray for several cloud top mixed-phase penetrations through a growing deep convective cloud on 27 January 2009 (top). Bottom panels illustrate CIP particle images for penetrations at (a)  $-5^{\circ}$ , and (b)  $-13^{\circ}\text{C}$ . The vertical axis of a CIP image panel represents 1.55 mm.

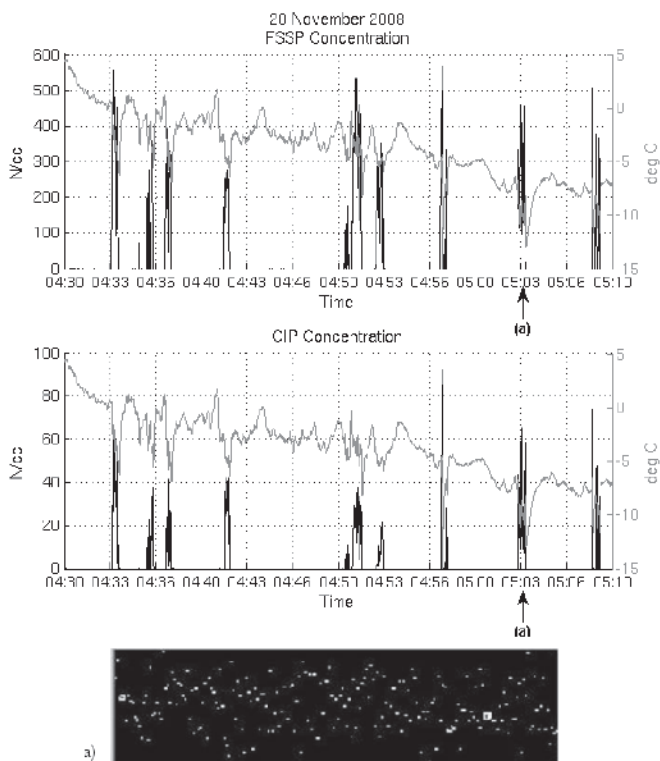


Figure 8. Same as Figure 7, except for 20 November 2008. CIP image shown in (a) is from a convective cloud top penetration at  $-9^{\circ}\text{C}$ .

### 3.2 Randomized seeding experiment

Sixty-two randomized cases were declared in season one and 65 in season two. A map of the location for all randomized cases declared between the two seasons is shown in Figure 9.

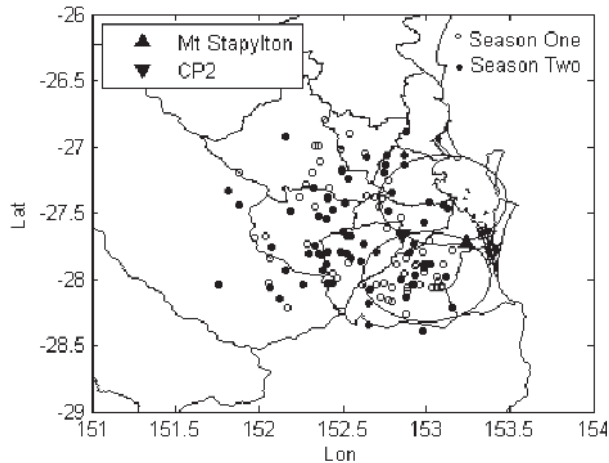


Figure 9. Map of the locations of all randomized seeding cases declared in season one (open circles) and season two (closed circles). Mt Stapylyton and CP2 radar locations are overlaid (see legend) along with the 30-degree dual-Doppler lobes that intersect at each radar.

Based on the statistical analysis criteria (set to match that used for the South African and Mexican experiments; see Section 2.2.3), 39 (19 seeded and 20 unseeded) of the 127 total randomized cases were included in the statistical analysis. The first season was dominated by days with shallow trade-wind cumulus clouds, and many of those randomized cases never developed a 35 dBZ echo that lived long enough (>2 volume scans) for inclusion in the statistical analysis. From our climatology analysis (see Section 2.2.1) and field experience from season one, we learned that less precipitation, especially from deep mixed-phase convection, occurs in March, while more deep convection can occur earlier in the season (beginning as early as October). Therefore, we shifted our field season up a month for season two, beginning in November and ending in February. As a result, we encountered more deep convection, increasing both the number of randomized cases meeting the statistical analysis criteria and in situ mixed-phase microphysical measurements. Furthermore, from our experiences in season one (and reinforced by our analysis from season one presented briefly in Section 3.1), we observed a lack of supercooled liquid water in the deep stratiform and most deep convective clouds in the region due to naturally efficient ice formation processes. Hence, there is little

opportunity for glaciogenic seeding in these situations. Therefore, we focused solely on randomized hygroscopic seeding in season two, whereas we had pursued some experimental (non-randomized) glaciogenic seeding in season one.

One of the major obstacles in the statistical analysis of rainfall enhancement experiments, such as the Queensland CSRP, has always been the effect of initial biases and outliers (large storms) that could easily overwhelm and dominate the statistical results. In addition, the effects of merging or splitting storms can influence and complicate the analysis substantially. Several such cases of storm mergers into large outliers were observed in the Queensland CSRP data set.

To study the effects of such large storms on the analysis, we stratified the storms by maximum volume. It is clear that most of the storms attained maximum volumes less than 1000 km<sup>3</sup> and that the seeded and unseeded storms were nearly equally represented in this sample (Fig. 10). For storms with maximum volumes between 1000 and 2000 km<sup>3</sup>, however, more seeded cases were observed while virtually no unseeded were. Conversely, more unseeded storms were observed with maximum volumes larger than 2000 km<sup>3</sup> than seeded clouds. This bias in not having equal representation of seeded and unseeded storms at larger volumes can impact the statistical analysis and emphasizes the importance of choosing appropriate statistical techniques to analyze the differences between seeded and unseeded storms. Our preliminary statistical analyses indicate that it is extremely important to take these effects into account when interpreting the results. In addition, it is important to note that for most storms larger than 1000 km<sup>3</sup>, mergers and splits introduce unrealistic storm tracks into the analysis. Consistent with the findings of Mather et al. (1997), we conclude that the statistical analysis and interpretation should focus on the storms that are less than 750 km<sup>3</sup> in volume because they exclude large merged complexes and line storms.

The analyses are still in progress, but initial results for the 39 cases that satisfied the statistical analysis criteria seem to indicate similar tendencies (although not statistically significant) for the radar-derived<sup>1</sup> rain mass, area, precipitation flux, and integrated precipitation mass to what was found in the South African and Mexican experiments (see rain mass results in Fig. 11; Mather et al. 1997, Foote and Brientjes 2000). At first glance one could easily interpret these results to suggest that hygroscopic seeding has a positive effect on rain mass,

<sup>1</sup> Single-polarization radar data (Mt Stapylyton) was used to derive these parameters, as was done in the South African and Mexican experiments.

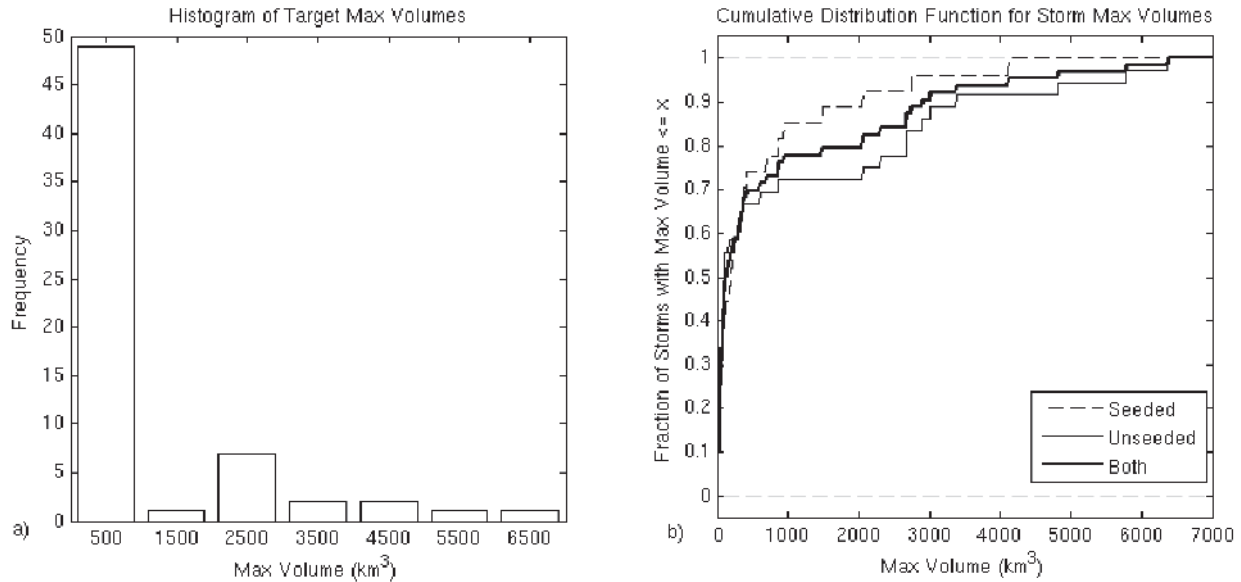


Figure 10. (a) Frequency histogram of TITAN tracks >35 dBZ, and (b) normalized frequency distribution of seeded, unseeded and total storm tracks as a function of maximum volume of tracks.

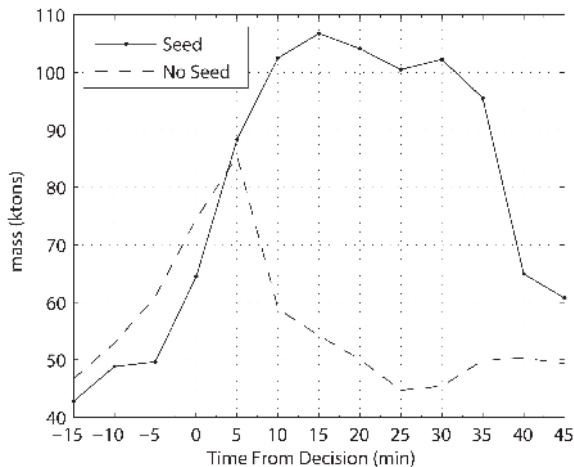


Figure 11. Radar-derived rain mass of the 35-dBZ echo as a function of time from 15 minutes prior to seeding decision time to 45 minutes after decision time for seeded (solid) and unseeded (dashed) cases.

but in some re-analyses we found that with such a small sample set, including or excluding cases by changing the selection criteria changed the results dramatically (not shown). The p-values (determined by the re-randomization test; not shown) should also be interpreted with caution because of multiplicity effects and the small sample size.

The only significant difference between the seeded and unseeded clouds in the re-randomization tests was for the duration of the clouds after seeding, with the seeded clouds living significantly longer than

the unseeded clouds (p-value of 0.04; not shown). This is also a similar result as to what was found in the South African and Mexican experiments.

#### 4. UNIQUE OPPORTUNITIES AND ONGOING ANALYSIS

##### 4.1 Dual-polarization and dual-wavelength radar studies

Dual-polarization and dual-wavelength measurements from the CP2 radar can offer unique insight into the microphysical properties and evolution of seeded and unseeded clouds. For example, the differential radar reflectivity ( $Z_{DR}$ ) is a polarimetric variable related to the size of raindrops (Bringi et al. 1986, Wakimoto and Bringi 1988, Brandes et al. 2004). In addition, particle identification in mixed phase processes is possible with dual-polarization radar (Vivekanandan et al. 1999). Furthermore, utilizing the ground-based disdrometer measurements, microphysical properties within the storms—such as drop median volume diameter ( $D_0$ ) and maximum drop diameter ( $D_{max}$ )—can be estimated using relationships derived from the radar reflectivity and differential reflectivity data (see Fig. 12). Such relationships have been calculated using the NCAR 2DVD disdrometer measurements from season one for convective and stratiform rains over the disdrometer (not shown). These measurements could provide new insights in the difference of microphysical processes between seeded and unseeded clouds.

Polarimetric radar measurements from CP2 are expected to be especially sensitive to the development of warm rain, and hence to hygroscopic seeding effects. If seeding significantly alters the raindrop size distribution, it should be detectable with polarimetric radar. Another possible radar-detectable response to cloud microphysical processes related to cloud seeding is the time to the development of precipitation. Here, the dual-wavelength capability of CP2 may play an important role. At 10 cm (S-band), the radar reflectivity needs to be above about 5 dBZ (occasionally as high as 10 dBZ) before one can be sure that it is caused by precipitation (Knight and Miller 1993). This is because Bragg scattering from turbulent mixing inside the clouds also produces radar echoes of this magnitude. However, at X-band (3 cm), this threshold is 20 dB lower such that when the reflectivity is above  $-15$  to  $-10$  dBZ it can be relied upon to be from water drops. Thus the X-band radar echo can be used to estimate cloud lifetime, while the S-band can be used to estimate a time when precipitation starts forming. If hygroscopic seeding is done early enough in a cloud's life cycle, there is the potential to see its effect with radar, both through the time required for precipitation formation and the early comparison of  $Z$  and  $Z_{DR}$ .

Another possible analysis technique to utilize the dual-polarization radar data is to statistically compare polarimetric characteristics of seeded cells with nearby similar unseeded cells (here we refer to them as "sister cells"). For this type of analysis, it would be important to select convective clouds that were fairly isolated, at a similar stage in their life cycle, and in which the seeding occurred at a similar stage of growth. By choosing single cell storms containing primarily one updraft, it should maximize the chance to observe any seeding modifications by reducing the likelihood that raindrops from nearby updrafts would mask events in the seeded updraft. This kind of effort could also utilize dual-Doppler analyses to ascertain the portions of the seeded cells that are more likely influenced by the seeding material (see following section).

#### 4.2 Dual-Doppler analysis

Having multiple Doppler radars scanning the same area allows for the radial velocities from each radar to be combined to estimate the three-dimensional winds within storms in the area (see Fig. 12). These overlapping coverage areas are often called dual-Doppler lobes, and such lobes (highlighting the area of 30 degree minimum beam crossing angles between the CP2 and Mt Stapylton radars) are illustrated in Fig. 1. Several storms were observed during the Queensland CSRP within the dual-Doppler lobes. Detailed polarimetric and dual-Doppler radar and aircraft-based analyses of these storms

will allow trajectories of seeding material to be determined and evaluation of the storms' microphysical and dynamical responses. The dual-Doppler analyses could also be used to initialize a cloud parcel model to study aerosol uptake in precipitating systems (both background and flare produced), as well as study the dynamical evolution (e.g., updraft intensity with time) of seeded and unseeded clouds. It may be possible to conduct a statistical study comparing updraft and downdraft intensities in seeded and unseeded storms and look for evidence of dynamical seeding effects that may contribute to the initiation and/or enhancement of secondary convection.

## 5. CONCLUSIONS

Two seasons of field operations were conducted for the Queensland Cloud Seeding Research Program (CSRP), with the first season taking place between December 2007 and March 2008, and the second season between November 2008 and February 2009. Analysis efforts for the Queensland CSRP were focused on three major issues for the greater Brisbane region: understanding the weather and climate, characterizing the atmospheric aerosol and cloud microphysics, and assessing the impact of cloud seeding on rainfall. The data sets collected in the two field seasons are vast and unprecedented for a cloud seeding research project, and thus many varied research efforts can continue to utilize the Queensland CSRP data sets. The purpose of this paper was to present an initial overview of the Queensland CSRP field experiment and the research and analyses that are being pursued.

The wet season in Southeast Queensland occurs generally from November–February. Climatology clustering analysis quantified that Southeast Queensland can be divided into 'wet' and 'dry' weather regimes, with the 'wet' regimes occurring most in summer and the 'dry' regimes more in winter. The 'wet' regimes are as such responsible for the majority of the region's rainfall and include the northwesterly, 'moist' southeasterly, easterly, and westerly regimes.

During the early part of the summer season, when cloud bases are generally higher, our results suggest that coalescence is not active at heights below the freezing level, and as such ice multiplication may not occur and first ice may only form at temperatures colder than  $-12^{\circ}\text{C}$ . Hygroscopic seeding may be more effective in these clouds by providing earlier coalescence and possibly the onset of a more efficient ice process. Otherwise, clouds in Southeast Queensland generally seem to develop precipitation initially via the "warm rain" process that then results in a more efficient mixed-phase

process in deeper convective systems that extend above the freezing level. Seeding with hygroscopic flares could potentially enhance the “warm rain” process, but glaciogenic seeding would not be advised in these conditions because of sufficient concentrations of natural ice particles at temperatures below  $-5^{\circ}\text{C}$ . Our observations indicate that natural precipitation processes are very efficient in deep stratiform systems. Thus, neither hygroscopic nor

glaciogenic seeding may have a positive effect in these systems.

The randomized seeding statistical results seem to show the same tendencies that were observed in previous experiments in South Africa and Mexico, which used the same hygroscopic seeding techniques. Nonetheless, the sample size is still too small to make any meaningful conclusions. Efforts

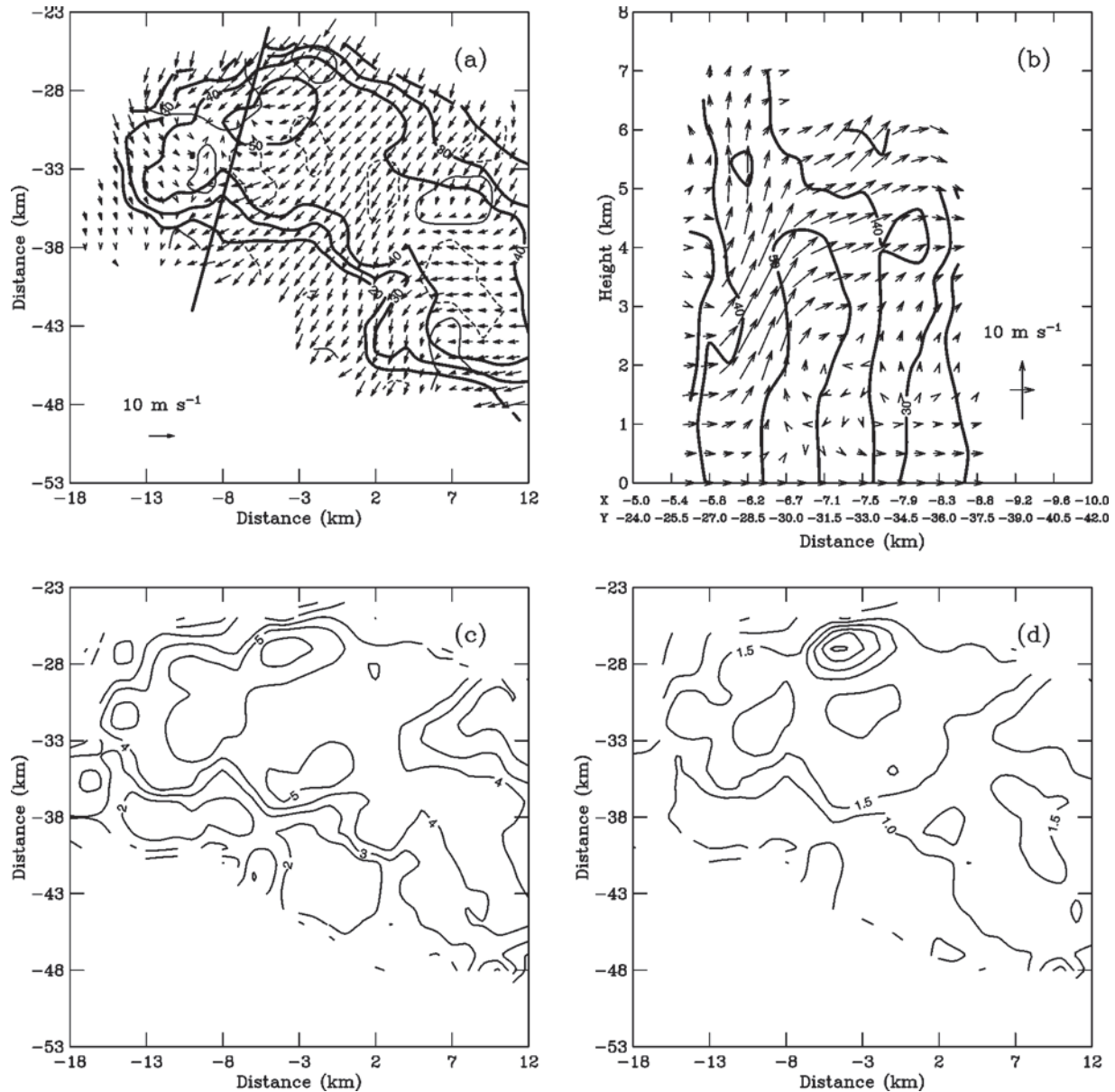


Figure 12. Example of multi-parameter radar analysis for a case observed in the 30-degree dual-Doppler lobes on 21 February 2009. (a) Horizontal cross section at 1 km and (b) vertical cross section through the plane highlighted in (a) of radar reflectivity contoured (thick black) with a 10-dBZ contour interval, and black arrows illustrate the wind vectors in the cross sectional plane from the dual-Doppler analysis. Thin black contours in (a) denote updrafts of  $1 \text{ m s}^{-1}$  (solid) and downdrafts of  $0.5 \text{ m s}^{-1}$  (dashed). Horizontal cross sections at 1 km of estimated (c) maximum drop diameter ( $D_{\text{max}}$ ; mm) and (d) median volume diameter ( $D_v$ ; mm) are also shown using relationships derived from disdrometer measurements (not shown).

are being made to use appropriate analysis techniques to interpret and understand the data and results. Future operations should focus on increasing the randomized sample size or attempt to design (a priori) a new confirmatory randomized experiment.

### 5.1 Future work

Given the vast amount of data collected in the two seasons of the Queensland CSR, there is a lot of analysis to be done. Efforts to utilize the polarimetric and dual-Doppler radar data for assessing the effects of cloud seeding are one of the key areas of future work, and will include developing innovative methods for this type of analysis. Furthermore, we plan to incorporate cloud resolving and parcel modeling into the analyses in order to corroborate and help explain the physical observations.

**Acknowledgements:** The Queensland Cloud Seeding Research Program was sponsored by the Queensland Government Department of Environment and Resource Management through the Queensland Climate Change Centre of Excellence (QCCCE). We acknowledge the tremendous efforts of the field project personnel who executed the field operations. Personnel were from NCAR, QCCCE, USQ, Monash University, BoM/CAWCR, SAWS, WITS, MIPD Pty Ltd, and WMI. The program design, execution, and subsequent scientific analysis are the result of collaborations with the above-mentioned institutions, as well as with Texas A&M University and Arizona State University. The Queensland CSR map (Figure 1) was produced by Kevin Sampson (NCAR). The authors gratefully acknowledge the NOAA Air Resources Laboratory (ARL) for the use of the HYSPLIT transport and dispersion model.

### REFERENCES

- Andreae, M.O., 2008: Correlation between cloud condensation nuclei concentration and aerosol optical thickness in remote and polluted regions. *Atmos. Chem. Phys. Discuss.*, **8**, 11293–11320.
- Brandes, E.A., G. Zhang and J. Vivekanandan, 2004: Drop size distribution retrieval with polarimetric radar: Model and application. *J. Appl. Meteor.*, **43**, 461–475.
- Bringi, V.N., R.M. Rasmussen and J. Vivekanandan, 1986: Multiparameter radar measurements in Colorado convective storms. Part I: Graupel melting studies. *J. Atmos. Sci.*, **43**, 2545–2563.
- Bringi, V., and A. Hendry, 1990: Technology of Polarization Diversity Radars for Meteorology. *Radar Meteorology*, David Atlas, Ed., Amer. Meteor. Soc., 153–190.
- Cleveland, H., 1978: *The Management of Weather Resources*. U.S. Government Printing Office, Washington D.C., 229 pp.
- Dixon, M. and G. Weiner, 1993: TITAN: Thunderstorm identification, tracking, analysis, and nowcasting—a radar-based methodology. *J. Atmos. Oceanic Technol.*, **10**, 785–797.
- Draxler, R.R., and G.D. Hess, 1998: An overview of the HYSPLIT\_4 modeling system for trajectories, dispersion, and deposition. *Aust. Meteor. Mag.*, **47**, 295–308.
- Foot, G.B., and R.T. Brintjes (eds.), 2000: WMO International Workshop on Hygroscopic Seeding: Experimental Results, Physical Processes, and Research Needs (1999: Mazatlán, México). World Meteorological Organization, WMP Report No. 35, WMO/TD No. 1006, Geneva, 68 pp.
- Hallet, J., and S.C. Mossop, 1974: Production of secondary ice crystals during the riming process. *Nature*, **249**, 26–28.
- Hartigan, J.A. and M.A. Wong, 1979: A K-means clustering algorithm. *Applied Stats.*, **28**, 100–108.
- Keenan, T., J. Wilson, J. Lutz, K. Glasson, and P. May, 2006: The restoration of CP2 in Brisbane, Australia. Preprints, *4<sup>th</sup> European Conf. on Radar in Meteorology and Hydrology (ERAD 2006)*, Barcelona, Spain, 367–370.
- Knight, C.A., and L.J. Miller, 1993: First radar echoes from cumulus clouds. *Bull. Amer. Meteor. Soc.*, **74**, 179–188.
- Levi, Y., and D. Rosenfeld, 1996: Ice nuclei, rainwater chemical composition and static cloud seeding effects in Israel. *J. Appl. Meteorol.*, **35**, 1494–1501.
- Mather, G.K., D.E. Terblanche, F.E. Steffens and L. Fletcher, 1997: Results of the South African cloud-seeding experiments using hygroscopic flares. *J. Appl. Meteor.*, **36**, 1433–1447.
- Peter, J.R., M.J. Manton, L. Wilson, S.M. Collis, P.T. May, and R. Potts, 2010: Radar-derived characteristics of storms in South East Queensland. *J. Appl. Meteor. Climatol.*, in review.
- Rosenfeld, D., and W.L. Woodley, 1993: Effects of cloud seeding in West Texas: Additional results and new insights. *J. Appl. Meteorol.*, **32**, 1848–1866.
- Vivekanandan, J., S. Ellis, R. Oye, D. Znić, A. Ryzhkov, and J. Straka, 1999: Cloud microphysics retrieval using S-band dual-polarization radar measurements. *Bull. Amer. Meteor. Soc.*, **80**, 381–388.
- Wakimoto, R.M. and V.N. Bringi, 1988: Dual-polarization observations of microbursts associated with intense convection: The 20 July storm during the MIST Project. *Mon. Wea. Rev.*, **116**, 1521–1539.